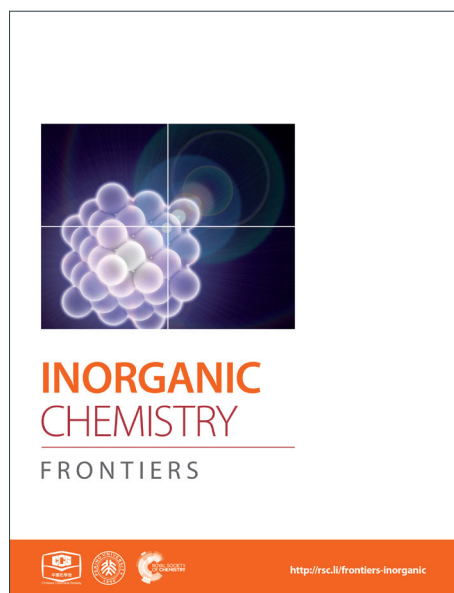
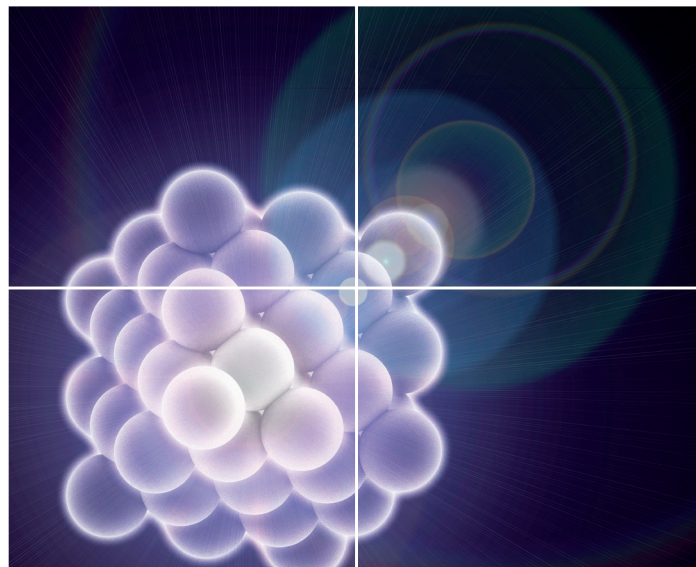


INORGANIC CHEMISTRY

FRONTIERS

Accepted Manuscript



This is an *Accepted Manuscript*, which has been through the Royal Society of Chemistry peer review process and has been accepted for publication.

Accepted Manuscripts are published online shortly after acceptance, before technical editing, formatting and proof reading. Using this free service, authors can make their results available to the community, in citable form, before we publish the edited article. We will replace this *Accepted Manuscript* with the edited and formatted *Advance Article* as soon as it is available.

You can find more information about *Accepted Manuscripts* in the [Information for Authors](#).

Please note that technical editing may introduce minor changes to the text and/or graphics, which may alter content. The journal's standard [Terms & Conditions](#) and the [Ethical guidelines](#) still apply. In no event shall the Royal Society of Chemistry be held responsible for any errors or omissions in this *Accepted Manuscript* or any consequences arising from the use of any information it contains.

Multichromophoric di-anchoring sensitizers incorporating a ruthenium complex and an organic triphenyl amine dyad have been constructed, which convert light to electrical energy with higher power conversion efficiency and incident-photon-to-current efficiency than the devices made of individual inorganic and organic dyes.

Received 00th January 20xx,
Accepted 00th January 20xx

DOI: 10.1039/x0xx00000x

rsc.li/frontiers-inorganic

Pei-Yang Su,^a Jun-Min Liu,^{*a} Xue-Lian Lin,^a Yi-Fan Chen,^a Yong-Shen,^a Li-Min Xiao,^b Dai-Bin Kuang^a and Cheng-Yong Su^{*a}

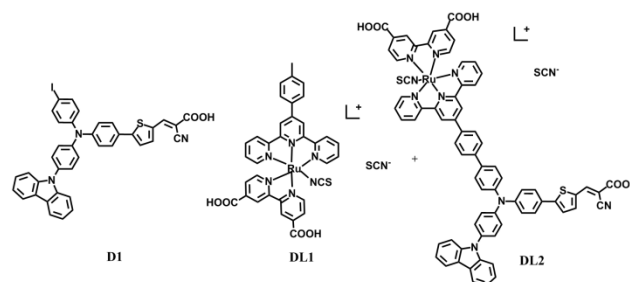
Multichromophoric dye-sensitized solar cells (DSSCs) based on the dual sensitization with a metal-organic combinatorial dye comprised of a ruthenium complex and an organic triphenyl amine dyad have been constructed, which convert light to electrical energy with higher power conversion efficiency and incident-photon-to-current efficiency than the devices made of individual inorganic and organic dyes.

Dye-sensitized solar cells (DSSCs) have gained considerable attention due to their relatively low manufacturing costs, high cell performance, and good mechanical flexibility.¹ Sensitizers, as crucial components in DSSCs, are responsible for the light harvesting and electron injection. The key tunable factors to obtain high efficiency dyes are to maximize the light-harvesting efficiency as well as to reduce charge recombination.² Despite convenient structural modifications, most of dyes developed thus far consist of uniform chromophore units, either metal complexes or metal-free organic dyes, that can absorb light only at limited wavelength regions, leaving the rest of the visible light essentially unused for energy conversion.³ To circumvent this problem, co-sensitization strategies were investigated by a combination of two or more dyes sensitized together on a semiconductor film.⁴ Many co-sensitization systems are reported to show enhanced photovoltaic performance relative to their individual single-dye systems.⁵ However, the physical mixing of different dyes in DSSCs may cause the complexity of cell assembly and the low cell stability to limit their practical application.

To improve the efficiency of DSSCs, there are some successful cases by using multi-anchoring organic dyes with

bridging groups to link up several D- π -A chains.⁶ Recently, we have developed a new class of calix[4]arene-based dyes containing four light-harvesting units and four anchoring groups per molecule, which enhanced molar extinction coefficients, promoted electron transfer between the dye and surrounding TiO₂, and increased the stability of the dyes adsorbed on the TiO₂ film.⁷ Wang et al reported di-anchoring organic dyes with bridging aromatic units and found the introduction of the bridging unit could suppress the charge recombination and minimize the dye aggregation.⁸ Therefore, such a new design approach becomes a useful direction for improving light-harvesting ability and electron injection efficiency.

In this study, a novel di-anchoring sensitizer **DL2** (Scheme 1) containing a benzene spacer which bridges one starburst triarylamine-based organic dye and one terpyridine-based ruthenium sensitizer was designed and synthesized. Analogous ruthenium sensitizer **DL1** and organic dye **D1**⁹ were also synthesized for comparison. The cell study results indicate that the di-chromophoric and di-anchoring dyes **DL2** can produce significantly higher value of short-circuit current density (J_{sc}), thus giving higher conversion efficiency (η). This new combinatorial dye exhibits higher light-harvesting efficiencies than individual dyes, which have been verified by UV-vis spectra and incident photon-to-current conversion efficiency (IPCE) measurements.



Scheme 1 Structures of combination dye **DL2** and comparison dyes **D1** and **DL1**.

^aMOE Laboratory of Bioinorganic and Synthetic Chemistry, State Key Laboratory of Optoelectronic Materials and Technologies, Lehn Institute of Functional Materials, School of Chemistry and Chemical Engineering, Sun Yat-Sen University, Guangzhou 510275, China. Fax: +86-20-84115178; Tel: +86-20-84115178; Email: liujunm@mail.sysu.edu.cn, cecscy@mail.sysu.edu.cn

^bSchool of Computer Science and Engineering, Beihang University, Beijing 100191, China

‡Electronic supplementary information (ESI) available: Detailed synthetic procedures of the **D1**, **DL1** and **DL2**, FTIR spectra of dye powders and dyes adsorbed on TiO₂ nanoparticles for **DL2**, their cyclic voltammetry Figures, absorption and electrochemical data, and photovoltaic parameters of the cosensitization DSSCs can be found in the ESI.

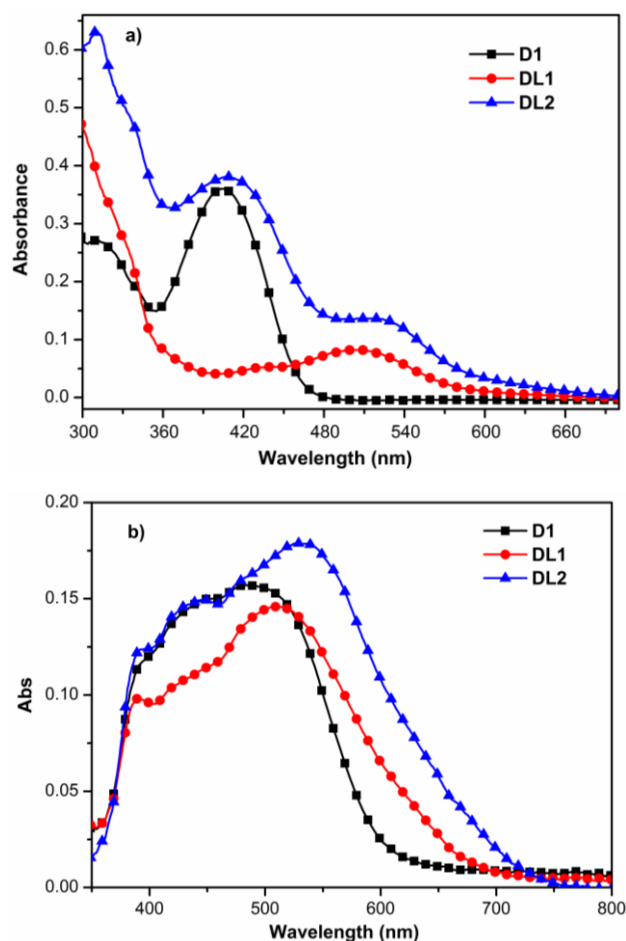


Fig. 1 The absorption spectra of **D1**, **DL1**, and **DL2** (a) in DMF solution and (b) on TiO_2 .

The synthetic details of **DL1** and **DL2** are described in the supporting information (Scheme S1). The precursors with one terpyridine and one aldehyde group were synthesized through a Suzuki coupling reaction. Then, the di-anchoring groups were introduced via a Knoevenagel condensation reaction and followed by reacting $\text{RuCl}_3 \cdot 3\text{H}_2\text{O}$ and 4,4'-dicarboxylic acid-2,2'-bipyridine (dcbpyH_2). The chemical structures were characterized by ^1H NMR, ^{13}C NMR, and ESI-MS.

As expected, the absorption spectrum of **DL2** in DMF (Fig. 1a) exhibits two distinct broad absorption peaks in the wavelength ranges of 350–450 nm and 450–600 nm, which is essentially a linear combination of the **D1** and **DL1** spectra, indicating that the HOMO-LUMO gaps of the individual dyes remain virtually unchanged in the dyad. **DL2** containing two light-harvesting units exhibits broader absorption than **D1** and **DL1**, which can improve its light-harvesting ability. In addition, the dyes **DL2** show higher molar absorption coefficients than **D1** and **DL1**. Upon adsorption onto the nanocrystalline TiO_2 films, the absorption peaks of the three dyes (Fig. 1b) are significantly broadened, which is favorable for light harvesting. The broader absorption of **DL2** compared with **D1** and **DL1** confirmed anchoring of the dyes onto TiO_2/FTO surfaces, which is consistent with their absorption spectra in DMF.

Furthermore, since **DL2** has much larger molecular size than **D1** and **DL1**, the

Table 1 Character Table of calculated excitation energies and composition in terms of molecular orbital contributions for **DL2**.

state (nm)	characters		
	occupied orbitals	empty orbitals	contributions (%)
S_1 (520)	HOMO-1	LUMO	91.9%
S_2 (415)	HOMO	LUMO+1	96.1%

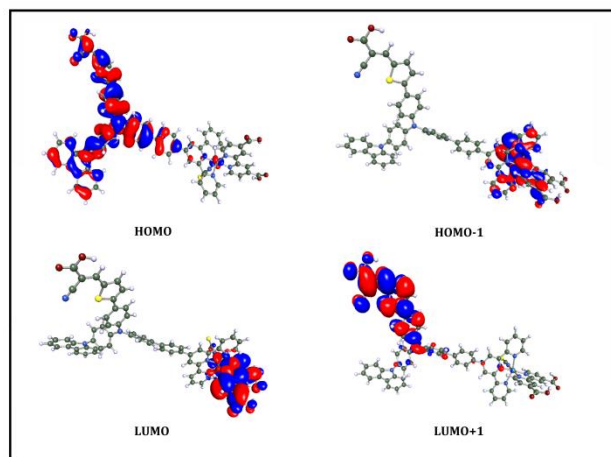


Fig. 2 Computed isosurface plots of selected Kohn-Sham molecular orbitals (from HOMO-1 to LUMO+1) of **DL2**.

dye loading amounts for **DL2** are slightly lower.

To elucidate the electronic properties of **DL2** further, we have performed theoretical calculations using both density functional theory (DFT) for the ground-state geometries and time-dependent DFT (TDDFT) for the excited-state energies and properties (see Computational Details in supporting Information). The computed data are listed in Table 1 and relevant occupied and unoccupied Kohn-Sham molecular orbitals of **DL2** involved in the transitions are shown in Fig. 2. It is found the first lowest-lying electronic transition, S_1 (mainly HOMO-1 \rightarrow LUMO), is directly charged from the ruthenium-NCS unit to the carboxy pyridine ligand bound to the TiO_2 surface in the inorganic part of **DL2**. In contrast, the S_2 (mainly HOMO \rightarrow LUMO+1) shows an apparent intramolecular charge transfer (ICT) between the triphenylamine-based donor and the cyanoacrylic acid in the organic part of **DL2**. This is consistent with the experiment absorption spectrum results.

The FT-IR spectra of the **DL2** dyes have been measured to study the binding ability of the dye attached to the TiO_2 surface.¹⁰ Fig. S1 shows the FTIR spectra of the dye powders and the dyes adsorbed on TiO_2 . For the powders of **DL2**, the C=O stretching bands of carboxylic acids (COOH) in 4-picolinic acids and 2-cyanoacrylic acids were observed at 1720 and 1654 cm^{-1} , respectively. When the dyes were adsorbed on TiO_2 surface, the C=O stretching bands at 1720 and 1654 cm^{-1} disappeared and instead two new peaks at 1713 and 1644 cm^{-1}

were found. This indicates deprotonation of two types of COOH groups in **DL2** dyes taking place on the TiO₂ surface.

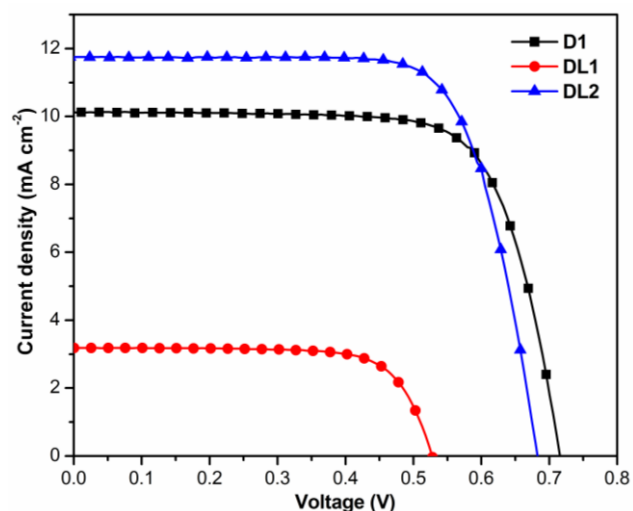


Fig. 3 Current-voltage characteristics of **D1**-, **DL1**-, and **DL2**-sensitized solar cells under AM 1.5 G simulated solar light (100 mW cm⁻²)

Cyclic voltammetry was performed for **D1**, **DL1** and **DL2** (Fig. S2) and the energy levels of the highest occupied molecular orbital (HOMO) and lowest unoccupied molecular orbital (LUMO) derived from the oxidation potentials and absorption/emission data (Fig. S3) of three dyes are summarized in Table S1. All the HOMO levels of the dyes are within -5.93 to -5.79 eV, which are much higher than the energy level of the conduction band of TiO₂ (-4.4 eV), providing the possibility of electron injection. The LUMO levels were observed to be within the range of -3.86 to -3.11 eV, which are lower than the iodide/triiodide redox potential value (-4.9 eV), indicating that the oxidized dyes could be regenerated by the electrolyte.

DSSCs were fabricated using **D1**, **DL1**, and **DL2** as the sensitizers, with an active area of 0.16 cm², nanocrystalline anatase TiO₂ particles, and the electrolyte composed of 0.6 M 1-methyl-3-propylimidazolium iodide, 0.10 M guanidinium thiocyanate, 0.03 M I₂, 0.5 M *tert*-butylpyridine in acetonitrile and valeronitrile (85:15, v/v). The current density-voltage (*J*-*V*) curves (Fig. 3) of the DSSCs fabricated from these dyes were measured under simulated AM 1.5G irradiation (100 mW cm⁻²), with the photovoltaic parameters summarized in Table 2. The **DL2**-based device displays much higher *J*_{sc} (11.75 mA cm⁻²) and *η* (5.84%) than those comprised of **D1** and **DL1** dyes (Table 2). This comparison clearly shows that the **DL2** dyad converts light to electricity much more efficiently than individual dyes. However, dye **DL2**-sensitized cell has a lower open-circuit

Table 2 Performance parameters of **D1**-, **DL1**-, and **DL2**-sensitized solar cells.

dye	<i>J</i> _{sc} /mA cm ⁻²	<i>V</i> _{oc} /mV	<i>FF</i>	<i>η</i> (%)
D1	10.13	752	0.75	5.45
DL1	3.18	536	0.73	1.23

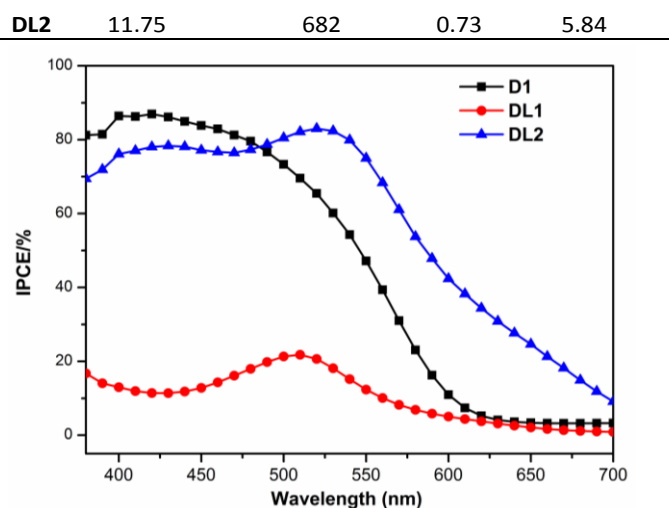


Fig. 4 Photocurrent action spectra of **D1**-, **DL1**-, and **DL2**-sensitized solar cells under AM 1.5 G simulated solar light (100 mW cm⁻²)

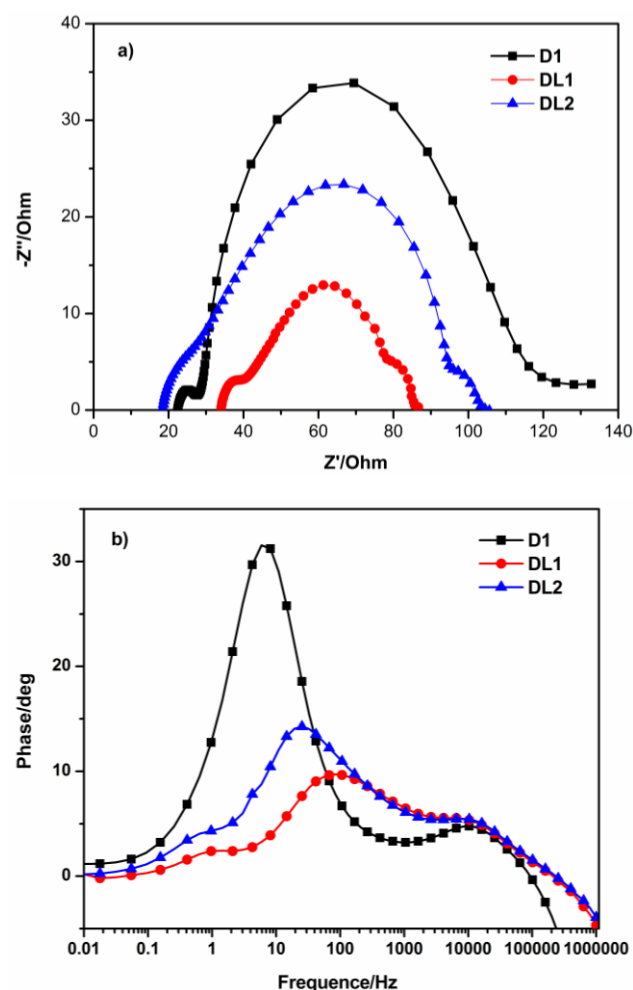


Fig. 5 Electrochemical impedance spectra (a) Nyquist plot and (b) Bode plot of DSSCs for **D1**, **DL1**, and **DL2** dyes.

voltage (V_{oc}) than that of **D1**, for DSSCs using **DL2** dye show shorter electron lifetime, as described in the following paragraph.

To elucidate the difference between the J_{sc} values, the incident photon-to-current conversion efficiencies (IPCEs) for the DSSCs based on the three dyes are shown in Fig. 4. The IPCEs of **D1** and **DL1** dyes show a band in the region of 380–620 nm with values of 82% at 410 nm and 20% at 510 nm, respectively. It is interesting that **DL2** with **D1** and **DL1** dye combination displays a broader and red-shifted band with a plateau between 400 and 560 nm with an IPCE value of over 79%, indicating that incorporation of a ruthenium complex and an organic triphenyl amine dye can effectively lead to enhanced DSSC cell currents.

Electrochemical impedance spectroscopy (EIS) analysis was performed to explain the different V_{oc} values obtained for the DSSCs based on **D1**, **DL1** and **DL2**. The interfacial charge transfer resistance (R_{ct}) and the electron lifetime (τ) could be acquired by fitting the EIS spectra.¹¹ As shown in the Nyquist plots (Fig. 5a), the R_{ct} values decrease in the sequence of **D1**>**DL2**>**DL1**, and the fitted τ values decrease in the order of **D1**>**DL2**>**DL1**, indicating the same order of decreasing charge recombination rate and increasing electron lifetime, which is consistent with that of the V_{oc} values. The Bode phase plots shown in Fig. 5b likewise support the differences in the electron lifetime for TiO₂ films based on the three dyes. The increase in the lifetime in the TiO₂ film is associated with a pronounced rise in the charge transfer resistance, which depends on the dye structure and adsorption number on TiO₂.¹² The V_{oc} of **D1** is higher than that of **DL1**, because the hydrophobic groups, such as carbazole, triarylamine, and thiophene units, might be beneficial for retarding the electron transfer from TiO₂ to the electrolyte, which would increase the electron lifetime and enhance the open circuit voltage. The lower V_{oc} for the **DL2** dyad was attributed mostly to the lower packing density of dyes on TiO₂ compared to **D1** dyes, which would result in the higher I_3^- concentration in the vicinity of the TiO₂ surface and smaller charge recombination resistance.

Intensity modulated photocurrent spectroscopy (IMPS) and intensity modulated photovoltage spectroscopy (IMVS) were carried out to further investigate the different photovoltaic behaviors of three dyes. Fig. 6a shows recombination time (τ_r) of DSSCs based on **D1**, **DL1**, and **DL2** dyes under various incident light intensities. The results indicate that the recombination time of the devices displays a systematic trend **D1**>**DL2**>**DL1**, consistent with the EIS results described above. On the other hand, the electron transport time (τ_d) of DSSCs based on the three dyes increases in the order **DL1**>**DL2**>**D1** as shown in Fig. 6b. Considering the interaction with the dye and electrolyte, we deduced it could be the reason that **DL1** and **DL2** having [Ru(L)(dcbpyH₂)NCS]⁺ structure might limit the access to the surface by Li⁺ ions which are known to assist the electron diffusion along the TiO₂ network, resulting in a slow photo-injected electron transport to FTO glass.¹³

To compare the physical co-sensitization effects of **DL1** and **D1** with our chemically integrated combinatorial dye on the cell performance, the photoanode TiO₂ films were first

immersed in the dye solution of **DL1** for 6h. Then, they were immersed in **D1** dye solutions for 6h, 9h, and 12h, respectively. The co-sensitized devices produce the photovoltaic efficiency

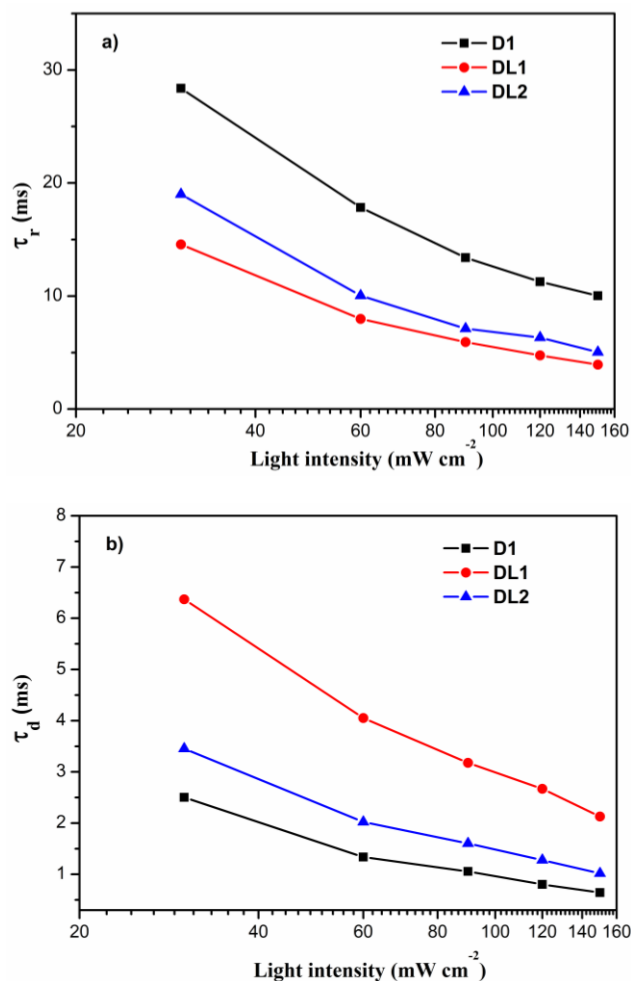


Fig. 6 (a) Incident light intensity dependent recombination time constants, (b) incident light intensity dependent transport time constants for DSSCs for **D1**, **DL1**, and **DL2** dyes.

of 3.78%, 4.43%, and 4.94%, respectively, which are significantly decreased with respect to **D1** dye alone under the same condition (Table S2), respectively. The results indicate that the physical co-sensitization of **DL1** and **D1** is not able to maximize the device's performance as the chemically combinatorial dye does, implying that synergistic co-sensitization effect from dyes combination is complicated, and chemical integration of metal-organic dyes might provide an alternative way for efficient dye-sensitized solar cells.

Conclusions

We have demonstrated that DSSCs based on metal-organic combinatorial dye can be constructed by introducing multichromophoric di-anchoring dyads **DL2** as the light-harvesting materials. On account of broad absorption cross-sections, **DL2**-based DSSCs display higher J_{sc} , η , and IPCE under standard conditions than those made of individual dyes. To the

best of our knowledge, this is the first example of chemically combinatorial dye incorporating a ruthenium complex and an organic triphenyl amine dye for efficient dye-sensitized solar cells. The combination strategy of inorganic and organic dyes offers an alternative way for the construction of more efficient DSSCs in which multiple electron donors, acceptors, and chromophores can be organized in an orderly fashion to facilitate red-shifted absorptions as well as high absorptivity for increased device efficiency.

Acknowledgements

This work was supported by NSF of China (21272292, 21450110063, 91222201), NSF of Guangdong Province (S2013030013474, 2011J2200053), and Special Research Found for the Doctoral Program of Higher Education (20120171130006).

Notes and references

- (a) B. O' Regan, M. Grätzel, *Nature*, 1991, **353**, 737-740; (b) B. O' Regan, J. R. Durrant, *Acc. Chem. Res.*, 2009, **42**, 1799-1808; (c) H. Ren, H. Shao, L. Zhang, D. Guo, Q. Jin, R. Yu, L. Wang, Y. Li, Y. Wang, H. Zhao, D. Wang, *Adv. Energy Mater.*, 2015, DOI: 10.1002/aenm.201500296; (d) Z. Dong, H. Ren, C. M. Hessel, J. Wang, R. Yu, Q. Jin, M. Yang, Z. Hu, Y. Chen, Z. Tang, H. Zhao, D. Wang, *Adv. Mater.*, 2014, **26**, 905-909; (e) L. Yi, Y. Liu, N. Yang, Z. Tang, H. Zhao, G. Ma, Z. Su, D. Wang, *Energy Environ. Sci.*, 2013, **6**, 835-840.
- (a) A. Hagfeldt, G. Boschloo, L. Sun, L. Kloo, H. Pettersson, *Chem. Rev.*, 2010, **110**, 6595-6663; (b) S. Ahmad, E. Guillèn, L. Kavan, M. Grätzel, M. K. Nazeeruddin, *Energy Environ. Sci.*, 2013, **6**, 3439-3466; (c) L. Martín-Gomis, F. Fernández-Lázaro, Á. Sastre-Santos, *J. Mater. Chem. A*, 2014, **2**, 15672-15682; (d) F. Gao, Y. Wang, D. Shi, J. Zhang, M. Wang, X. Jing, R. Humphry-Baker, P. Wang, S. M. Zakeeruddin, M. Grätzel, *J. Am. Chem. Soc.*, 2008, **132**, 10720-10728.
- (a) A. J. Mozer, P. Wagner, D. L. Officer, G. G. Wallace, W. M. Campbell, M. Miyashita, K. Sunahara and S. Mori, *Chem. Commun.*, 2008, 4741-4743; (b) C. Huang, S. Barlow and S. Marder, *J. Org. Chem.*, 2011, **76**, 2386-2407; (c) B. E. Hardin, H. J. Snaith and M. D. McGhee, *Nat. Photonics*, 2012, **6**, 162.
- (a) S. Chang, H. Wang, Y. Hua, Q. Li, X. Xiao, W. K. Wong, W. Y. Wong, X. Zhu and T. Chen, *J. Mater. Chem. A*, 2013, **1**, 11553-11558; (b) X. Sun, Y. Wang, X. Li, H. Ågren, W. Zhu, H. Tian, Y. Xie, *Chem. Commun.*, 2014, **50**, 15609-15612.
- (a) C. M. Lan, H. P. Wu, T. Y. Pan, C. W. Chang, W. S. Chao, C. T. Chen, C. L. Wang, C. Y. Lin, E. W. G. Diau, *Energy Environ. Sci.*, 2012, **5**, 6460-6464; (b) C. L. Wang, J. Y. Hu, C. H. Wu, H. H. Kuo, Y. C. Chang, Z. J. Lan, H. P. Wu, E. W. G. Diau, C. Y. Lin, *Energy Environ. Sci.*, 2014, **7**, 1392-1396.
- (a) C.-H. Siu, L. T. L. Lee, P.-Y. Ho, P. Majumdar, C.-L. Ho, T. Chen, J. Zhao, H. Lie, W.-Y. Wong, *J. Mater. Chem. C*, 2014, **2**, 7086-7095; (b) D. Cao, J. Peng, Y. Hong, X. Fang, L. Wang, H. Meier, *Org. Lett.*, 2011, **13**, 1610-1613.
- L.-L. Tan, J.-M. Liu, S.-Y. Li, L.-M. Xiao, D.-B. Kuang, C.-Y. Su, *ChemSusChem.*, 2015, **8**, 280-287.
- X. Ren, S. Jiang, M. Cha, G. Zhou, Z.-S. Wang, *Chem. Mater.*, 2012, **24**, 3493-3499.
- L.-L. Tan, H.-Y. Chen, L.-F. Hao, Y. Shen, L.-M. Xiao, J.-M. Liu, D.-B. Kuang, C.-Y. Su, *Phys. Chem. Chem. Phys.*, 2013, **15**, 11909-11917.
- Z.-S. Wang, K. Hara, Y. Dan-oh, C. Kasada, A. Shinpo, S. Suga, H. Arakawa, Hideki Sugihara, *J. Phys. Chem. B*, 2005, **109**, 3907-3914.
- L.-L. Tan, J.-F. Huang, Y. Shen, L.-M. Xiao, J.-M. Liu, D.-B. Kuang, C.-Y. Su, *J. Mater. Chem. A*, 2014, **2**, 8988-8994.
- Z. Ning, Y. Fu, H. Tian, *Energy Environ. Sci.*, 2010, **3**, 1170-1181.
- S. Kambe, S. Nakade, T. Kitamura, Y. Wada, S. Yanagida, *J. Phys. Chem. B*, 2002, **106**, 2967-2972.